Supporting Information to :

Three-dimensional reconstruction of liquid phases in disordered mesopores using in situ small-angle scattering

Cedric J. Gommes*

The present document provides mathematical and data analysis details that supplement the main text. The specific pieces of information to which explicit reference is made in the main text are the following

- The Wide-Angle X-ray Scattering (WAXS) patterns measured on the same sample as in Figure 2 of the main text are shown in Figure SI-1 on page 2;
- The increased in Q that would result from a phase separation is calculated in Section I A, particularly in Eqs. SI-9 and SI-10;
- The general mathematical expression for the specific interface areas in terms of a line integral in the (Y, Z) plane is Eq. SI-51;
- The determination of the Gaussian random field wave vector distribution compatible with the SAXS pattern of the empty RF gel is explained in Section II A;
- The calculation of the SAXS intensity of the plurigaussian model is explained in section II B, together with the least-square fit procedure;
- The values of the raw parameters b, β and l_Z of the plurigaussian model obtained by least-square fit are shown in Fig. SI-4 on page 13.

CONTENTS

* cedric.gommes@ulg.ac.be

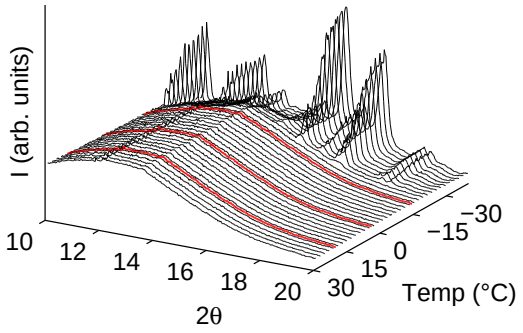

FIG. SI-1. The Wide-Angle X-ray Scattering (WAXS) patterns measured on the RF gel imbibed with critical nitrobenzene/hexane solution show that the pore-filling phases remain liquid above -15 °C. The three highlighted temperatures are the same as on Figure 2 of the main text, namely, T = 20, 5 and -14 °C.

I. MATHEMATICAL DETAILS

A. General expression for the SAXS intensity of three-phase systems

The Small-Angle X-ray Scattering (SAXS) signal results from the spatial variability (at a nanometer-scale) of the electron density $\rho(x)$ of the investigated system. The latter variability is described quantitatively through the correlation function $C(r)$, defined as

$$C(r) = \langle(\rho(\mathbf{x}+\mathbf{r}) - \langle\rho\rangle)(\rho(\mathbf{x}) - \langle\rho\rangle)\rangle \tag{SI-1}$$

where $\langle . \rangle$ stands for the average value, calculated over all possible $\mathbf{x}$. We have assumed here that the sample is statistically isotropic, so that $C(\mathbf{r})$ depends only on the modulus $r = |\mathbf{r}|$.

The SAXS intensity, expressed as a function of q, is the 3D Fourier transform of $C(r)$, which can be put under the form

$$I(q) = \int_0^\infty \frac{\sin(qr)}{qr} C(r) 4\pi r^2 \, dr \tag{SI-2}$$

Practically, the intensity that is measured experimentally $I^*(q)$ is proportional to $I(q)$

$$I^*(q) = K \; I(q) \tag{SI-3}$$

where K is a constant that depends on the intensity of the beam, the scattering cross-section, the volume of the system that is irradiated, etc.

We shall assume that the system can be approximated as being made up of three phases, each having a uniform electron density. In the case we are considering, these phases are the solid (density ρ_S) and the two pore-filling phases: one is the nitrobenzene-rich phase A (with density ρ_A) and the other is the hexane-rich phase B (with density ρ_B). With this approximation, the electron density spatial correlation function can be written as [1]

$$\begin{aligned} C(r) = {} & (\rho_S - \rho_A)(\rho_S - \rho_B)\left[P_{SS}(r) - \phi_S^2\right] + (\rho_A - \rho_S)(\rho_A - \rho_B)\left[P_{AA}(r) - \phi_A^2\right] \\ & + (\rho_B - \rho_S)(\rho_B - \rho_A)\left[P_{BB}(r) - \phi_B^2\right] \end{aligned} \tag{SI-4}$$

where the functions $P_{SS}(r)$, $P_{AA}(r)$ and $P_{BB}(r)$ are the two-point probability functions of phases S, A, and B [2]. These functions are equal to the probability that two points randomly chosen in the system at distance r from each other both belong to phase S, A or B, respectively.

An important quantity for SAXS data analysis is the total scattered intensity Q (the so-called Porod's invariant [3]) which is defined as

$$Q = \int_0^\infty I(q) 4\pi q^2 \, dq \tag{SI-5}$$

TABLE SI-1. Physical characteristics of the molecules in their pure state. The characteristics of the solid phase of the RF gel were determined assuming an overall stoichiometry $C_8H_{7.33}O_{2.66}$, and the solid density ρ_m measured by helium pycnometry on the desiccated gel.

	ρ_m (g/mL)	M (g/mol)	N_e (e^-)	v_m (mL/mol)	ρ ($e^-/Å^3$)
Nitrobenzene	1.199	123	64	102.59	0.38
Hexane	0.65	86	50	131.34	0.23
RF solid	1.5	146	76.67	97.33	0.47

ρ_m: mass density, M: molar mass, N_e: number of electrons in the molecule, v_m: molar volume, ρ: electron density.

The value taken by Q for a three-phase system is obtained by calculating the inverse Fourier transform of , yielding

$$C(r) = \frac{1}{(2\pi)^3} \int_0^\infty \frac{\sin(qr)}{qr} I(q) 4\pi q^2 \, \mathrm{d}q \tag{SI-6}$$

and evaluating this integral for $r \to 0$. This leads to

$$\begin{aligned} \frac{Q}{(2\pi)^3} = &(\rho_S - \rho_A)(\rho_S - \rho_B)\left[\phi_S - \phi_S^2\right] + (\rho_A - \rho_S)(\rho_A - \rho_B)\left[\phi_A - \phi_A^2\right] \\ &+ (\rho_B - \rho_S)(\rho_B - \rho_A)\left[\phi_B - \phi_B^2\right] \end{aligned} \tag{SI-7}$$

where we have used Eq. SI-4 and we have taken into account that the two-point function $P_{XX}(r)$ of any phase X satisfies

$$P_{XX}(r \to 0) = \phi_X \tag{SI-8}$$

where ϕ_X is the volume fraction of the phase.

Equation SI-7 shows that the total scattered intensity depends only on the volution fractions and the electron densities of all phases. In particular, Q is a constant during a morphological transition that keeps the composition and the volumes of all phases unchanged. This is also true of $Q^* = KQ$, which is measurable experimentally. We shall come back to this is section II.

The electron densities of the various molecules present are derived in Tab. SI-1. In the case of the solid phase of the RF gel, it was assumed to have the stoichiometry $C_8H_{7.33}O_{2.66}$ [4]. Its mass density was assumed 1.5 g/mL, which is the value commonly measured by helium pycnometry on the xerogel, obtained after desiccating the gel.

If we assume as in the main text that the overall composition of the pore-filling liquid is 50 vol. % hexane and 50 vol. % nitrobenzene, the electron density of pore-filling liquid would be $\bar{\rho} \simeq 0.3$ $e^-/Å^3$. This value is simply the average of ρ_N and ρ_H, as given in Tab. SI-1. Using that value, the total scattered intensity is calculated from Eq. SI-7 with $\rho_A = \rho_B = \bar{\rho}$, yielding

$$\frac{Q_{\text{homogeneous}}}{(2\pi)^3} = (\rho_S - \bar{\rho})^2 \phi_S (1 - \phi_S) \simeq 0.0054 \tag{SI-9}$$

where $\phi_S = 0.24$ is the volume fraction of the solid.

By contrast, if the pore-filling liquid would demix into two pure phases with electron densities ρ_N and ρ_H, and volume fractions $\phi_A = \phi_B = (1 - \phi_S)/2$, the total scattered intensity would take the value

$$\frac{Q_{\text{phase separated}}}{(2\pi)^3} \simeq 0.0095 \tag{SI-10}$$

according to Eq. SI-7. This corresponds to a 75 % increase, compared to a homogeneous pore-filling solution. A phase separation of the pore-filling liquid is therefore easily measurable in our experimental systems.[5]

B. Electron densities of the pore-filling phases

We shall refer to the pore filling phases as A and B, and they contain Nitrobenzene (N) and Hexane (H) in various proportions. The purpose of the present section is to propose a parametrization of the composition of phases A and B that is compatible with the known global composition of the pore-filling liquids. That parametrization is then used to estimate the electron densities ρ_A and ρ_B of the two phases.

We shall build on a previous modeling of SAXS analysis of phases with changing compositions [6], and we assume that the any exchange of matter between the two phases preserve the total volume. Accordingly, it is useful to describe the composition of the phases through the volume fractions x_N^A, x_N^B, x_H^A, x_H^B of molecules N and H in phases A and B.

The volume fractions satisfy

$$\begin{aligned} x_N^A + x_N^B &= x_N \qquad x_H^A + x_H^B = x_H \\ x_N^A + x_H^A &= \varphi_A \qquad x_N^B + x_H^B = \varphi_B \end{aligned} \tag{SI-11}$$

where we have used the notation x_N and x_H for the volume fraction of N and H ($x_H + x_N = 1$), and φ_A and φ_B for the volume fraction of phases A and B *relative to the pore volume*. In other words

$$\varphi_A = \phi_A/(\phi_A + \phi_B) \quad \text{and} \quad \varphi_B = \phi_B/(\phi_A + \phi_B) \tag{SI-12}$$

where ϕ_A and ϕ_B are the volume fractions of phases A and B.

With these notations, the electron densities of the two phases are written as

$$\rho_A = \frac{\rho_N x_N^A + \rho_H x_H^A}{\varphi_A} \quad \rho_B = \frac{\rho_N x_N^B + \rho_H x_H^B}{\varphi_B} \tag{SI-13}$$

These equations are used to calculate the SAXS intensity.

Note that the composition of the two phases is completely described through the four volume fractions used in SI-11. However, only three of the four equations in SI-11 are independent. Once x_N, x_H, φ_A and φ_B are specified, an additional parameter is needed to describe the composition of the two phases. We define parameter ϵ as follows:

$$x_N^A = \begin{cases} x_N\varphi_A + \epsilon\ x_N\varphi_B & \text{for} \quad \epsilon \geq 0 \\ x_N\varphi_A + \epsilon\ x_N\varphi_A & \text{for} \quad \epsilon < 0 \end{cases} \tag{SI-14}$$

This definition is motivated by the fact that $\epsilon = 0$ corresponds to $x_N^A = x_N\varphi_A$, i.e., to both phases having the same composition. The value $\epsilon = 1$ corresponds to $x_N^A = x_N$, i.e. phase A is pure N. By contrast, for $\epsilon = -1$ one has $x_N^A = 0$, i.e., phase A is pure H.

The variable ϵ can be thought of as a measure of the phase separation, which is complete for either $\epsilon = +1$ or $\epsilon = -1$. However, these two values are not necessarily realizable, depending of the relative values of $\varphi_{A/B}$ and $x_{H/N}$. To investigate this, let us calculate the other three volume fractions through the use of Eq. SI-11. This leads to

$$\begin{aligned} x_H^A &= \begin{cases} x_H\varphi_A - \epsilon\ x_N\varphi_B & \text{for} \quad \epsilon \geq 0 \\ x_H\varphi_A - \epsilon\ x_N\varphi_A & \text{for} \quad \epsilon < 0 \end{cases} \\ x_N^B &= \begin{cases} x_N\varphi_B - \epsilon\ x_N\varphi_B & \text{for} \quad \epsilon \geq 0 \\ x_N\varphi_B - \epsilon\ x_N\varphi_A & \text{for} \quad \epsilon < 0 \end{cases} \\ x_H^B &= \begin{cases} x_H\varphi_B + \epsilon\ x_N\varphi_B & \text{for} \quad \epsilon \geq 0 \\ x_H\varphi_B + \epsilon\ x_N\varphi_A & \text{for} \quad \epsilon < 0 \end{cases} \end{aligned} \tag{SI-15}$$

The upper and lower bounds on ϵ are obtained by imposing

$$0 \leq x_{N/H}^{A/B} \leq \min\left\{x_{N/H}\ ,\ \varphi_{A/B}\right\} \tag{SI-16}$$

which leads to the following condition on ϵ

$$\epsilon_{\text{inf}} \leq \epsilon \leq \epsilon_{\text{sup}} \tag{SI-17}$$

with

$$\epsilon_{\text{inf}} = \max\left\{-1, -\frac{\varphi_B\ x_H}{\varphi_A\ x_N}\right\} \quad \text{and} \quad \epsilon_{\text{sup}} = \min\left\{+1, +\frac{\varphi_A\ x_H}{\varphi_B\ x_N}\right\} \tag{SI-18}$$

Given the global composition of the pore-filling phases (through x_N and x_H), and their volume fractions (through φ_A and φ_B), any value of ϵ can be chosen in the bounds defined by Eq. SI-17. Introducing this value in Eqs. SI-14 and SI-15, the composition of each phase is calculated. Knowing the compositions, the electron densities are finally calculated through Eq. SI-13.

C. Plurigaussian morphological models

1. *Gaussian random fields*

The central concept in plurigaussian models is that of Gaussian random field. A Gaussian random field $Y(\mathbf{x})$ can be obtained as a sum of random waves, as follows

$$Y(\mathbf{x}) = \sqrt{\frac{2}{N}} \sum_{n=1}^{N} \cos(\mathbf{q}_n \cdot \mathbf{x} + \phi_n) \tag{SI-19}$$

with $N \to \infty$. In this equation $\mathbf{q}_n$ and ϕ_n are random vectors and phases. The phases are uniformly distributed over in $[0, 2\pi)$, and the wavevectors are distributed according to a three-dimensional function $f_Y(\mathbf{q})$ normalized as

$$\int f_Y(\mathbf{q})\ \mathrm{d}\mathbf{q} = 1 \tag{SI-20}$$

where the integral is over the entire $\mathbf{q}$ space. The case considered in the main text is that of an isotropic GRF, for which $f_Y(\mathbf{q})$ is a radial function. We shall consider here the general case.

The field $Y(\mathbf{x})$ is entirely characterized by the corresponding wave-vector distribution function. Knowing the latter is equivalent to knowing the field-field correlation function $g_Y(r)$, defined as

$$g_Y(\mathbf{r}) = \langle Y(\mathbf{x}) Y(\mathbf{x} + \mathbf{r}) \rangle \tag{SI-21}$$

where the brackets stand for the average value calculated over all $\mathbf{q}$'s and ϕ's. The GRF being stationary, the average can also be calculated over $\mathbf{x}$.

The value of $Y(\mathbf{x})$ for any $\mathbf{x}$ is Gaussian distributed, with mean 0. Moreover, the the factor $\sqrt{2/N}$ in Eq. (SI-19) ensures that the variance of $Y(x)$ is 1. The joint distribution of the values taken by $Y(\mathbf{x})$ at two positions $\mathbf{x}_1$ and $\mathbf{x}_2$ at distance $\mathbf{r}$ from each other is a bivariate Gaussian distribution with mean 0, variance 1, and correlation coefficient $g_Y(\mathbf{r})$.

Using standard trigonometric manipulations, the following relation between $g_Y(\mathbf{r})$ and $f_Y(\mathbf{q})$ is obtained from Eq. SI-19

$$g_Y(\mathbf{r}) = \int f_Y(\mathbf{q}) \cos\left(\mathbf{q} \cdot \mathbf{r}\right)\ \mathrm{d}\mathbf{q} \tag{SI-22}$$

in the limit where $N \to \infty$. In the particular case of isotropic GRFs, the distribution of $\mathbf{q}$ does only depend on the modulus $q = |\mathbf{q}|$. In this case the relation is simply

$$g_Y(r) = \int_0^\infty f_Y(q) \frac{\sin\left(qr\right)}{qr}\ 4\pi q^2 \mathrm{d}q \tag{SI-23}$$

For further purposes, it is useful to analyze the small-distance behavior of $g_Y(r)$. This is done in the general anisotropic case by developing $\cos(\mathbf{q} \cdot \mathbf{r})$ in a Taylor series. This leads to following quadratic expression

$$g_Y(\mathbf{r}) \simeq 1 - \mathbf{r}^T \mathbf{L}_\mathbf{Y}^{-\mathbf{2}} \mathbf{r} \tag{SI-24}$$

where $\mathbf{L}_\mathbf{Y}^{-\mathbf{2}}$ is the following second order tensor

$$\mathbf{L}_\mathbf{Y}^{-\mathbf{2}} = \frac{1}{2} \int f_Y(\mathbf{q})\ \mathbf{q} \otimes \mathbf{q}\ \mathrm{d}\mathbf{q}\ . \tag{SI-25}$$

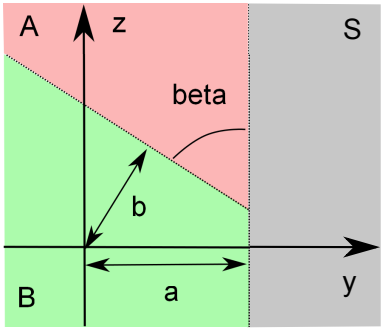

FIG. SI-2. Partitioning of the (Y, Z) plane corresponding to the plurigaussian model used in the main text, with three phases A (red), B (green), and S (gray), and the definition of the parameters a, b and β.

where $\otimes$ is the dyadic product. In the case where the GRF is isotropic, the asymptotic expression for $g_Y(r)$ reduces to

$$g_Y(r) \simeq 1 - \left(\frac{r}{l_Y}\right)^2 \tag{SI-26}$$

with

$$\frac{1}{l_Y^2} = \frac{1}{6}\int_0^\infty f_Y(q) q^2 \; 4\pi q^2 \mathrm{d}q \tag{SI-27}$$

This result can also be obtained by developing $\sin(qr)/(qr) \simeq 1 - (qr)^2/6$ in Eq. SI-23.

2. *Volume fractions and two-point correlation functions of Plurigaussian models*

The plurigaussian model used in the main text is based on two independent Gaussian random fields, $Y(\mathbf{x})$ and $Z(\mathbf{x})$, each of which is defined by a specific wave-vector distribution $f_Y(k)$ and $f_Z(k)$. The values taken by the two GRFs at any given point of space can be represented as a (Y, Z) plane. A given phase, say phase n, is modeled as a region D_n of the latter plane, as illustrated in Fig. 3 of the main text and in Fig. SI-2.

The volume fraction of phase n, ϕ_n, can be viewed as the probability that any given point $\mathbf{x}$ of space belongs to phase n. This can also be calculated as the total probability associated with the domain D_n is the (Y, Z) plane. Because Y and Z are both Gaussian distributed with average 0 and variance 1, the volume fraction is calculated as

$$\phi_n = \int_{D_n} \mathrm{d}y\mathrm{d}z \; \frac{1}{2\pi} \exp\left[-\frac{y^2+z^2}{2}\right] \tag{SI-28}$$

This integral can be simplified in the particular case where the domain D_n is a half-plane, defined by a single threshold as

$$D_S = \{(Y, Z) | Y \geq a\} \tag{SI-29}$$

The solid phase S in the main text is defined in such a way (see Fig. SI-2). In this case, Eq. SI-28 becomes

$$\phi_S = \frac{1}{\sqrt{2\pi}} \int_a^\infty \exp\left(-\frac{y^2}{2}\right) \; \mathrm{d}y \tag{SI-30}$$

The two-point correlation function $P_{mn}(\mathbf{r})$ is defined as the probability that two random points $\mathbf{x}_1$ and $\mathbf{x}_2$ belong to phase m and n, respectively, with $\mathbf{x}_2 - \mathbf{x}_1 = \mathbf{r}$. This probability can be calculated using the fact that values $Y(\mathbf{x}_1)$ and $Y(\mathbf{x}_2)$ obey a Gaussian bivariate distribution with mean 0, variance 1 and correlation function $g_Y(\mathbf{r})$. The same applies to $Z(\mathbf{x}_1)$ and $Z(\mathbf{x}_2)$ with correlation coefficient $g_Z(\mathbf{r})$. Accordingly, the two-point correlation function can be calculated as

$$P_{mn}(r) = \int_{(y_1,z_1)\in D_m} \mathrm{d}y_1\mathrm{d}z_1 \int_{(y_2,z_2)\in D_n} \mathrm{d}y_2\mathrm{d}z_2 \; G_{g_Y(\mathbf{r})}(y_1, y_2) G_{g_Z(\mathbf{r})}(z_1, z_2) \tag{SI-31}$$

where G_g is the bivariate Gaussian distribution with mean 0, variance 1 and correlation g, namely

$$G_g(x_1, x_2) = \frac{1}{2\pi\sqrt{1-g^2}} \exp\left[-\frac{x_1^2 + x_2^2 - 2g\ x_1 x_2}{2(1-g^2)}\right] \tag{SI-32}$$

For calculating the small-angle scattering patterns through Eq. SI-4, the general expression SI-31 has to be particularlized to $m = n = A$, to $m = n = B$, and to $m = n = S$.

In the particular case of phase S with domain D_S given by Eq. SI-29, Eq. SI-31 simplifies to the well-known result [7]

$$\begin{aligned} P_{SS}(\mathbf{r}) &= \phi_S^2 + \frac{1}{2\pi}\int_0^{g_Y(r)} \frac{1}{\sqrt{1-t^2}} \exp\left(\frac{-a^2}{1+t}\right)\ \mathrm{d}t \\ &= \phi_S^2 + \frac{1}{2\pi}\int_0^{\mathrm{asin}[g_Y(\mathbf{r})]} \exp\left(\frac{-a^2}{1+\sin(\theta)}\right)\ \mathrm{d}\theta \end{aligned} \tag{SI-33}$$

The second equation simply results from a change of variable $t = \sin(\theta)$, which leads to an expression that is easier to handle numerically because of the absence of the $1/\sqrt{1-t^2}$ singularity.

In the general case where the domains D_X has a shape that does not allow the integral in Eq. SI-31 to be calculated analytically, it is convenient to develop the bivariate Gaussian distributions as a series of Hermite's polynomial, as

$$G_g(x_1, x_2) = \sum_{n=0}^{\infty} \frac{g^n}{n!} H_n(x_1) H_n(x_2) \frac{1}{2\pi} \exp\left[-\frac{x_1^2 + x_2^2}{2}\right] \tag{SI-34}$$

where the Hermite polynomials are defined as

$$H_n(x) = (-1)^n e^{x^2/2} \frac{d^n}{dx^n}\left(e^{-x^2/2}\right) \tag{SI-35}$$

Using this development, the two-point correlation functions $P_{XX}(r)$ can be written as [8]

$$P_{XX}(r) = \sum_{n=0}^{\infty}\sum_{p=0}^{\infty} \frac{g_Y(r)^n}{n!} \frac{g_Z(r)^p}{p!} \Theta_{np}(X)^2 \tag{SI-36}$$

with

$$\Theta_{np}(X) = \int_{(y,z)\in D_X} H_n(y) H_p(z) \frac{1}{2\pi} \exp\left[-\frac{y^2 + z^2}{2}\right]\ \mathrm{d}y\mathrm{d}z \tag{SI-37}$$

3. Specific interface areas

The specific surface and interface areas can be calculated from the asymptotic behavior of the two-point correlation functions for small values of r [9–11]. In particular, the specific surface area of phase n, S_n is calculated as

$$S_n = -4\ \frac{\mathrm{d}P_{nn}(r)}{\mathrm{d}r}\bigg|_{r\to 0} \tag{SI-38}$$

and the specific interface area S_{mn} between phases m and n is calculated as

$$S_{mn} = 4\ \frac{\mathrm{d}P_{mn}(r)}{\mathrm{d}r}\bigg|_{r\to 0} \tag{SI-39}$$

Therefore, to calculate the specific surface area of a plurigaussian model it is necessary to estimate the two-point correlation function (Eq. SI-31) for vanishingly small distances r. When considering this limit, it is legitimate to express the correlation function g of the Gaussian random field as

$$g \simeq 1 - \epsilon^2 \tag{SI-40}$$

where ϵ is proportional to r, in agreement with Eq. SI-26. Under the assumption that ϵ is small, the bivariate Gaussian distribution in Eq. SI-32 can be approximated as

$$G_g(x_1,x_2) = \frac{1}{\sqrt{4\pi}} \exp\left(-\frac{1}{8}(x_1+x_2)^2\right) \frac{1}{\sqrt{2\pi\epsilon^2}} \exp\left(-\frac{1}{4\epsilon^2}(x_1-x_2)^2\right) + O(\epsilon^2) \tag{SI-41}$$

which we have factored as the product of two univariate distributions of (x_1+x_2) and of (x_1-x_2).

Using this approximation, the two-point correlation function (Eq. SI-31) can be approximated as

$$\begin{aligned} P_{mn}(r) \simeq \int_{(y_1,z_1)\in D_m} \mathrm{d}y_1\mathrm{d}z_1 \int_{(y_2,z_2)\in D_n} \mathrm{d}y_2\mathrm{d}z_2 \; \frac{1}{4\pi} \exp\left(-\frac{1}{8}(y_1+y_2)^2 - \frac{1}{8}(z_1+z_2)^2\right) \\ \frac{1}{2\pi\epsilon_Y\epsilon_Z} \exp\left(-\frac{1}{4\epsilon_Y^2}(y_1-y_2)^2\right) \exp\left(-\frac{1}{4\epsilon_Z^2}(z_1-z_2)^2\right) \end{aligned} \tag{SI-42}$$

where we have used the obvious notations $g_Y \simeq 1-\epsilon_Y^2$ and $g_Z \simeq 1-\epsilon_Z^2$.

We now proceed to rewrite Eq. SI-42 in a slightly different way, to show that the interface area can be calculated from an integral on the boundary of the domains D_m. For that purpose, let us do the following change of variable

$$\delta_y = y_1 - y_2 \quad \text{and} \quad \delta_z = z_1 - z_2 \tag{SI-43}$$

which leads to

$$\begin{aligned} P_{mn}(r) \simeq \int_{(y_1,z_1)\in D_m} \mathrm{d}y_1\mathrm{d}z_1 \int_{\mathbb{R}^2} \mathrm{d}\delta_y\mathrm{d}\delta_z \; i_n(y_1-\delta_y, z_1-\delta_z) \frac{1}{2\pi} \exp\left(-\frac{y_1^2+z_1^2}{2}\right) \\ \frac{1}{\sqrt{2\pi}\sigma_Y} \exp\left(-\frac{\delta_y^2}{2\sigma_Y^2} - \frac{\delta_y^2 - 4y_1\delta_y}{8}\right) \frac{1}{\sqrt{2\pi}\sigma_Z} \exp\left(-\frac{\delta_z^2}{2\sigma_Z^2} - \frac{\delta_z^2 - 4z_1\delta_z}{8}\right) \end{aligned} \tag{SI-44}$$

where $i_n(y,z)$ is the indicator function of D_n in (y,z) plane, defined as

$$i_n(y,z) = \begin{cases} 1 \;\text{ if } & (y,z) \in D_n \\ 0 \;\text{ otherwise} & \end{cases} \tag{SI-45}$$

In Eq. SI-44 we have written $\sigma_{Y/Z} = \sqrt{2}\epsilon_{Y/Z}$ to put the last two exponentials in a form closer to the canonical Gaussian. When $\sigma_{Y/Z}$ become vanishingly small the latter two functions converge to Dirac distributions of δ_y and δ_z. In that limit, one has simply

$$P_{mn}(r) \simeq \frac{1}{2\pi} \int_{(y_1,z_1)\in D_m} \mathrm{d}y_1\mathrm{d}z_1 \exp\left(-\frac{y_1^2+z_1^2}{2}\right) i_n^*(y_1,z_1) \tag{SI-46}$$

where

$$i_n^*(y_1,z_1) = \int_{\mathbb{R}^2} \mathrm{d}\delta_y\mathrm{d}\delta_z \; i_n(y_1-\delta_y, z_1-\delta_z) \frac{1}{2\pi\sigma_Y\sigma_Z} \exp\left(-\frac{\delta_y^2}{2\sigma_Y^2} - \frac{\delta_z^2}{2\sigma_Z^2}\right) \tag{SI-47}$$

is a blurred version of $i_n(y_1,z_1)$ in which the transition between 1 and 0 spreads over a region of thickness $\sigma_{Y/Z}$.

We shall now consider specifically the case where $m \neq n$. In this case, it has to be noted that the only values of $i_j^*(y_1,z_1)$ relevant for Eq. SI-46 are those outside of D_n. In that region, $i_n^*(y_1,z_1)$ is different from 0 only in thin layer of thickness $\sigma_{Y/Z}$ close to the boundary of D_n. When the layer becomes infinitely thin, i_n^* only depends on the distance ξ to the boundary through

$$i_n^*(\xi) = \frac{1}{\sqrt{2\pi}\sigma} \int_{\xi/\sigma}^{\infty} \exp(-x^2/2) \; \mathrm{d}x \tag{SI-48}$$

with

$$\sigma^2 = \sigma_Y^2 n_Y^2 + \sigma_Z^2 n_Z^2 \tag{SI-49}$$

where $n_{Y/Z}$ are the Y/Z components of the normal vector to the boundary of D_n. The integral of i_n^* per unit length of the boundary is therefore $\sigma/\sqrt{2\pi}$. Equation SI-46 takes therefore the final form

$$P_{mn}(r) = \frac{r}{2\pi^{3/2}} \int_{\partial D_{mn}} \exp\left(-\frac{y^2+z^2}{2}\right) \sqrt{\frac{n_Y^2}{l_Y^2} + \frac{n_Z^2}{l_Z^2}}\ \mathrm{d}l + O(r^2) \tag{SI-50}$$

where ∂D_{mn} is the common boundary of D_m and D_n. When deriving Eq. SI-50, we have taken into account that $\sigma_{Z/Z} = \sqrt{2}\frac{r}{l_{Y/Z}}$.

The specific interface area between phases m and n is then obtained as

$$S_{mn} = \frac{2}{\pi^{3/2}} \int_{\partial D_{mn}} \exp\left(-\frac{y^2+z^2}{2}\right) \sqrt{\frac{n_Y^2}{l_Y^2} + \frac{n_Z^2}{l_Z^2}}\ \mathrm{d}l \tag{SI-51}$$

The specific surface area of any phase n is obtained by summing the contribution of all phases it may be in contact with, i.e.

$$S_n = \sum_{m \neq n} S_{mn} \tag{SI-52}$$

This is equivalent to replacing the integral in Eq. SI-51 by an integral over

$$\partial D_n = \bigcup_{m \neq n} \partial D_{mn} \tag{SI-53}$$

i.e. over the total boundary of D_n.

With the parameters defined in Fig. SI-2, one finds that the specific area of the $A|B$ interface is

$$\boxed{S_{AB} = \frac{\sqrt{2}}{\pi} \sqrt{\left(\frac{\cos(\beta)}{l_Y}\right)^2 + \left(\frac{\sin(\beta)}{l_Z}\right)^2} e^{-b^2/2} \left\{1 - \mathrm{erf}\left(\frac{b\cos(\beta) - a}{\sqrt{2}\sin(\beta)}\right)\right\}} \tag{SI-54}$$

where $\mathrm{erf}(x)$ is the error function defined as

$$\mathrm{erf}(x) = \frac{2}{\sqrt{\pi}} \int_0^x e^{-t^2} dt \tag{SI-55}$$

The area of the $A|S$ interface is

$$\boxed{S_{AS} = \frac{\sqrt{2}}{\pi} \frac{e^{-a^2/2}}{l_Y} \left\{1 - \mathrm{erf}\left(\frac{b - a\cos(\beta)}{\sqrt{2}\sin(\beta)}\right)\right\}} \tag{SI-56}$$

and the area of the $B|S$

$$\boxed{S_{BS} = \frac{\sqrt{2}}{\pi} \frac{e^{-a^2/2}}{l_Y} \left\{1 + \mathrm{erf}\left(\frac{b - a\cos(\beta)}{\sqrt{2}\sin(\beta)}\right)\right\}} \tag{SI-57}$$

The total specific surface area of phase S is calculated as $S_{AS} + S_{BS}$. This leads to

$$S_S = \frac{2^{3/2}}{\pi} \exp\left(\frac{-a^2}{2}\right) \frac{1}{l_Y} \tag{SI-58}$$

which is the classical expression for a simple clipped Gaussian field [7].

II. DATA ANALYSIS

A. Reconstruction of the solid phase

We describe in the present section how the solid phase of the gel is reconstructed from the small-angle scattering data, using the clipped Gaussian field model. This procedure is used notably to produce the inset of Fig. 1 of the main text.

The volume fraction of the solid phase of the gel is related to the threshold a through the general relation given by Eq. SI-30. With the particular value $\phi_S = 0.24$, known from the composition of the gel, this leads to $a = 0.703$. Given the threshold a, the reconstruction of the gel morphology requires to determine the distribution of wave vectors $f_Y(k)$, or equivalently the field correlation function $g_Y(r)$.

When the gel is imbibed with pure nitrobenzene, the electron density correlation function $C(r)$ is simply proportional to the autocovariance function of the solid phase of the gel, i.e. to

$$\chi_S(r) = P_{SS}(r) - \phi_S^2 \tag{SI-59}$$

This results from Eq. SI-4 by setting $\rho_A = \rho_B = \rho_N$. Therefore, the SAXS intensity measured on the gel imbibed with pure nitrobenzene, $\tilde{I}(q)$, is proportional to the Fourier transform of $\chi_S(r)$.

The general relation between the field correlation function $g_Y(r)$ and the two-point function of the solid phase $P_{SS}(r)$ was given in Eq. SI-33. It can be written in terms of $\chi_S(r)$ as

$$\chi_S(r) = \frac{1}{2\pi} \int_0^{g_Y(r)} \frac{1}{\sqrt{1-t^2}} \exp\left(\frac{-a^2}{1+t}\right)\, dt \tag{SI-60}$$

The procedure we used to determine $f_Y(k)$ from $\tilde{I}(q)$ is similar to the one proposed by Quintanilla [12]. It is as follows.

1. Starting from the experimental SAXS pattern $\tilde{I}(q)$ of the gel imbibed with pure nitrobenzene, the autocovariance function of the solid phase is calculated through an inverse Fourier transform as

$$\tilde{\chi}_S(r) = \int_0^\infty \frac{\sin(qr)}{qr} \tilde{I}(q) 4\pi q^2\, dq \tag{SI-61}$$

   In practice, the SAXS intensity is measured only over a finite range: of $q_1 \leq q \leq q_2$. The data $\tilde{I}(q)$ have therefore to be extrapolated to calculate the integral. The large-q extrapolation is done by assuming Porod scattering of the type $\tilde{I}(q) \simeq A/q^4$ for $q \geq q_2$ [3] and the low-q extrapolation is done by assuming $\tilde{I}(q) \simeq Bq$ for $q \leq q_1$.

   This provides $\tilde{\chi}_S$ within an unknown multiplicative constant. The latter is obtained by imposing that $\tilde{\chi}_S(r = 0) = \phi_S(1 - \phi_S)$.

2. Once the threshold a is specified, Eq. SI-60 defines a reversible transformation between $g_Y(r)$ and $\chi_S(r)$. Using the calculated value of $\tilde{\chi}_S(r)$, Eq. SI-60 is inverted numerically for each particular r, yielding an estimated field correlation function $\tilde{g}_Y(r)$.

3. In general, the estimated field correlation function $\tilde{g}_Y(r)$ does not satisfy the necessary condition that it has to be positive-definite [13]. Therefore, we shall look for a positive-definite function that is as close as possible to $\tilde{g}_Y(r)$. This is done by minimizing

$$\int_0^\infty \left|\tilde{g}_Y(r) - g_Y(r)\right|^2 4\pi r^2\, dr \tag{SI-62}$$

   subject to the condition that $g_Y(r)$ be positive-definite.

   Taking advantage of Parseval's theorem, the latter functional can be conveniently written in Fourier space

$$\int_0^\infty \left|\tilde{f}_Y(q) - f_Y(q)\right|^2 4\pi q^2\, dq \tag{SI-63}$$

   where $\tilde{f}_Y(q)$ and $f_Y(q)$ are the Fourier transforms of $\tilde{g}_Y(r)$ and $g_Y(r)$, defined as in Eq. SI-23.

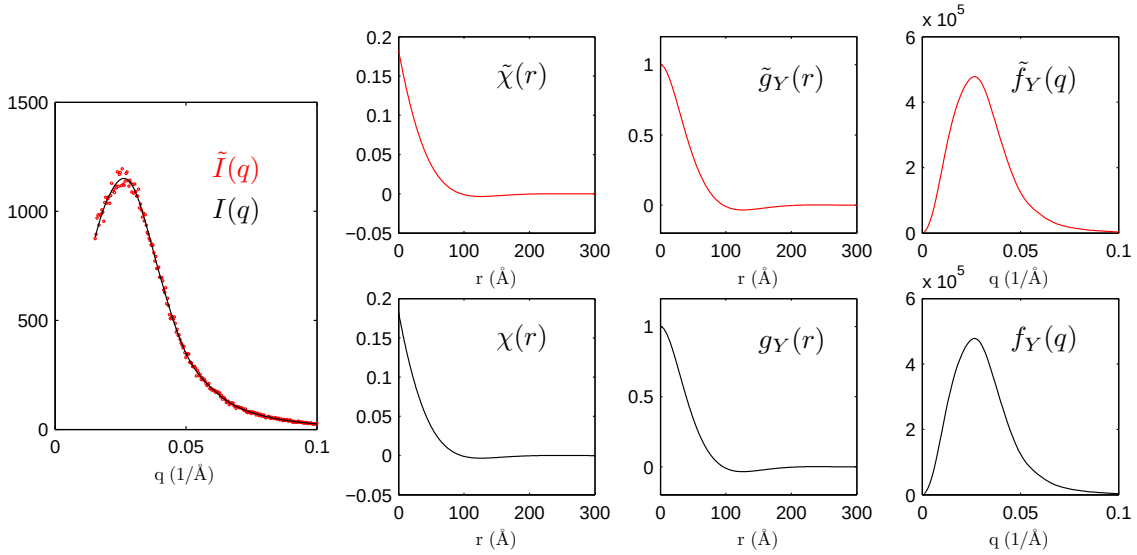

FIG. SI-3. Procedure for analyzing the empty solid as a clipped Gaussian random field. The Figure should be read clockwise (see text): Starting from the experimental SAXS pattern ($\tilde{I}(q)$, red dots) the functions $\tilde{\chi}(r)$, $\tilde{g}_Y(r)$ and $\tilde{f}_Y(q)$ are calculated successively; $f_Y(q)$ is then obtained by quadratic optimization, and $g_Y(r)$, $\chi(r)$, and $I(q)$ (solid black line) are calculated. The tilded and non-tilded functions are indistinguishable on the scale of the figure, which points to the accuracy of the model.

The problem therefore consists is determining the positive $f_Y(q)$ that minimize the quantity defined by Eq. SI-63 subject to the constraint

$$\int_0^\infty f_Y(q) 4\pi q^2 \, \mathrm{d}q = 1 \tag{SI-64}$$

The latter condition ensures that $g_Y(0) = 1$, i.e., that the variance of Y is equal to 1.

Expressing all the integrals with trapezoidal approximations, the minimization of Eq. SI-63 subject to $f_Y(q) \geq 0$ and to Eq. SI-64 is a classical case of quadratic programming. It was solved numerically using the Matlab ®optimization toolbox.

4. The field correlation function $g_Y(r)$ that best matches the experimental SAXS pattern of the solid is then obtained through an inverse Fourier transform of $f_Y(q)$. Once $g_Y(r)$ is known, the auto-covariance $\chi_S(r)$ is calculated by inverting Eq. SI-60, and $I(q)$ is calculated as the Fourier transform of $\chi_S(r)$. This enables one to check the accuracy of the reconstruction by comparing directly $I(q)$ with $\tilde{I}(q)$.

The entire procedure is illustrated in Fig. SI-3. The functions $\tilde{\chi}(r)$, $\tilde{g}_Y(r)$ and $\tilde{f}_Y(q)$ are indistinguishable from $\chi(r)$, $g_Y(r)$ and $f_Y(q)$ on the scale of the figure. This results from the fact that $\tilde{f}_Y(q)$ is already positive almost everywhere so that the effect of the quadratic optimization is minimal. This points to the excellent accuracy of the model in the case of RF gels.

B. Reconstruction of the pore-filling phases

The SAXS intensity is the Fourier transform of the electron density correlation function $C(r)$ given by Eq. SI-4, which can be written as

$$I^*(q) = K\Big[(\rho_S - \rho_A)(\rho_S - \rho_B) I_S(q) + (\rho_A - \rho_S)(\rho_A - \rho_B) I_A(q) + (\rho_B - \rho_S)(\rho_B - \rho_A) I_B(q)\Big] \tag{SI-65}$$

where we have used the notation

$$I_X(q) = \int_0^\infty \frac{\sin(qr)}{qr} \left[P_{XX}(r) - \phi_X^2\right] 4\pi r^2 \, dr \tag{SI-66}$$

for $I_S(q)$, $I_A(q)$ and $I_B(q)$.

The reconstruction of the pore-filling phases is done by least-square fit of the SAXS data with Eq. SI-65. We here list all the parameters of the model and how they are determined.

1. The constant K accounts for actual volume of the sample that is irradiated by x-rays, for the scattering cross-section of the molecules, etc. It is therefore expected to depend minimally on the temperature, we assume it is a constant all over the investigated temperature range. It is estimated once and for all as

$$K = \frac{Q^*}{Q_{\text{phase separated}}} \tag{SI-67}$$

   where Q^* is the experimental total scattered intensity (which is constant, see Fig. **??**) and $Q_{\text{phase separated}}$ has been introduced in Eq. SI-10.

2. All characteristics of the solid phase ρ_S, the threshold a, and $I_S(q)$ are known at this stage. The electron density ρ_S is given in Tab. SI-1, and $I_S(q)$ has been calculated in Sec. II A. Both are assumed to be temperature-independent.

3. The parameters that enter $I_A(q)$ and $I_B(q)$ are those of the plurigaussian model, i.e. parameter b and β defined in Fig. SI-2, as well as the wave-vector distribution of the Gaussian random field Z. The latter is modeled as

$$g_Z(r) = \exp\left[-\left(\frac{r}{l_Z}\right)^2\right] \tag{SI-68}$$

   which has a single parameter l_Z.

4. The composition of the pore-filling phases A and B, and hence their electron densities ρ_A and ρ_B, are entirely determined by a single parameter ϵ that quantifies the extent of the phase separation, as shown in Sec. I B. The two phases A and B have identical composition if $\epsilon = 0$, and phase A (B) is enriched in nitrobenzene for positive (negative) values of ϵ. During the exploratory phase of the research ϵ was used as an adjustable parameter, and the least-square fit systematically lead to the largest possible value of ϵ, i.e. $\epsilon = \epsilon_{\text{sup}}$ (see Eq. SI-18). In other words, the nitrobenzene content of phase A is always the largest possible, i.e.

$$\text{if} \quad \varphi_A < x_N \quad \text{then} \begin{cases} \rho_A = \rho_N \\ \rho_B = \left[\rho_H x_H + \rho_N (x_N - \varphi_A)\right] / \varphi_B \end{cases} \tag{SI-69}$$

   and

$$\text{if} \quad \varphi_A \geq x_N \quad \text{then} \begin{cases} \rho_A = \left[\rho_N x_N + \rho_H (\varphi_A - x_N)\right] / \varphi_A \\ \rho_B = \rho_H \end{cases} \tag{SI-70}$$

   In these equations, x_N and x_H are the known global volume fractions of nitrobenzene and hexane in the pores ($x_H = x_N = 0.5$), and $\varphi_{A/B} = \phi_{A/B}/(\phi_A + \phi_B)$ are calculated simply from parameters b and β. Therefore, the composition of the pore-filling phases does not introduce any independent parameter.

The least-square fit of $I^*(q)$ was done with b, β and l_Z as only adjustable parameters. The successive steps in the calculation of $I^*(q)$ are the following,

1. For any value of the parameters, the volume fractions $\phi_{A/B}$ are determined by numerically calculating the integral in Eq. SI-28.

2. This enables in turn to estimate the electron densities $\rho_{A/B}$ through Eqs. SI-69 and SI-70.

3. The two-point correlation functions $P_{AA}(r)$ and $P_{BB}(r)$ are calculated as a series of powers of $g_Y(r)$ and $g_Z(r)$ via Eq. SI-36, with 20 terms. The series converges for small values of $g_{Y/Z}$, i.e. for large values of r. By contrast, $g_{Y/Z}(r)$ is close to 1 for short distances r. For short distances, the two-point correlation functions are approximated as

$$P_{XX}(r) \simeq \phi_X - \frac{S_X}{4} r \tag{SI-71}$$

   where the specific surface areas are calculated via Eqs. SI-54, SI-56 and SI-57.

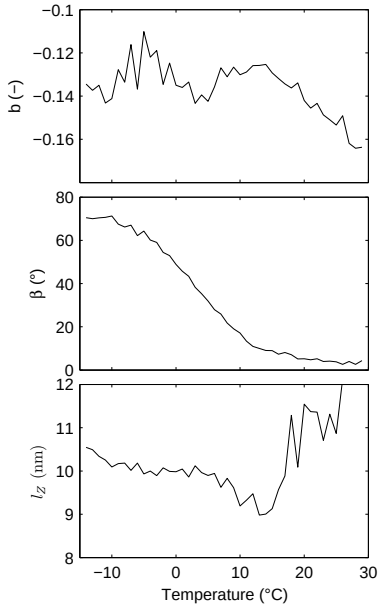

FIG. SI-4. Values of the plurigaussian parameters b, β and l_Z obtained by least-square fitting of the SAXS data. These are the values from which Fig. 6 of the main text was obtained.

4. Finally, the functions $I_A(q)$ and $I_B(q)$ are calculated numerically via Eq. SI-66, and introduced in Eq. SI-65 to yield $I^*(q)$.

In practice, the least-square minimization was done by starting at the lowest temperature $T = -14$ °C, and by using the values of b, β and l_Z towards which the minimization has converged at temperature T as the starting point for the minimization at temperature $T + 1$. The minimization was programmed in Matlab, using a Levenberg-Marquart algorithm. The values of parameters b, β and l_Z obtained in this way are plotted in Fig. SI-4.

[1] S. Ciccariello, G. Cocco, A. Benedetti, and S. Enzo, Physical Review B **23**, 6474 (1981).
[2] P. Debye, H. R. Anderson Jr., and H. Brumberger, Journal of Applied Physics **28**, 679 (1957).
[3] O. Glatter and O. Kratky, *Small Angle X-ray Scattering* (Academic Press, New York, 1982).
[4] S. A. Al-Muhtaseb and J. A. Ritter, Advanced Materials **15**, 101 (2003).
[5] If we assume the more conservative values 36 vol. % nitrobenzene and 64 vol. % hexane, the increase of Q resulting from phase separation is estimated to be 52 %, which is still largely measurable.
[6] C. J. Gommes, J. . Pirard, and B. Goderis, Journal of Physical Chemistry C **114**, 17350 (2010).
[7] P. Levitz, Adv. Colloid. Interf. Sci. **76**, 71 (1998).
[8] C. Lantuejoul, *Geostatistical modelling* (Springer, Berlin, 2000).
[9] J. Serra, *Image Analysis and Mathematical Morphology*, Vol. 1 (Academic Press, London, 1982).
[10] S. Torquato, *Random Heterogeneous Materials* (Springer, New York, 2000).
[11] M. Sahimi, *Heterogeneous Materials I: Linear Transport and Optical Properties*, Vol. 1 (Springer, New York, 2003).
[12] J. A. Quintanilla and W. M. Jones, Physical Review E - Statistical, Nonlinear, and Soft Matter Physics **75** (2007).
[13] N. F. Berk, Physical Review A **44**, 5069 (1991).